The energy-loss spectrum of extensive air showers recorded by the Haverah Park 500 m array

1969 J. Phys. A: Gen. Phys. 2 591

(http://iopscience.iop.org/0022-3689/2/5/012)

J. PHYS. A (GEN. PHYS.), 1969, SER. 2, VOL. 2. PRINTED IN GREAT BRITAIN

The energy-loss spectrum of extensive air showers recorded by the Haverah Park 500 m array

J. D. HOLLOWS, H. W. HUNTER and A. N. SURI†
Department of Physics, University of Leeds

MS. received 15*th January* 1969, *in revised form* 21*st May* 1969

Abstract. An integral energy-loss spectrum of air showers is presented for each of four zenith angle intervals 0°–20°, 20°–30°, 30°–35° and 35°–40°, based on 2950 showers selected from over 30 000 recorded by the Haverah Park 500 m air shower array in a running time of $6{\cdot}4 \times 10^7$ s. Here the energy loss of a shower is defined as the energy dissipated by the shower in an annulus of water 1·2 m thick in the range of distance 100 m to 1000 m from the shower axis.

The array consists of three water-filled Čerenkov detectors, each of area 34 m^2 and depth 1·2 m, symmetrically disposed at a radius of 500 m about a similar central detector. The mean altitude of the array is 220 m above sea level.

The energy-loss spectra for the four zenith angle intervals may be represented by power laws of exponent $-1{\cdot}94 \pm 0{\cdot}06$, $-2{\cdot}10 \pm 0{\cdot}06$, $-2{\cdot}26 \pm 0{\cdot}09$ and $-2{\cdot}22 \pm 0{\cdot}10$, respectively, over the energy-loss range $10^{14\cdot6}$–$10^{15\cdot6}$ ev. This corresponds, in so far as the relation between energy loss and primary energy has been established, to primary energies in the range 10^{17}–10^{18} ev.

The zenith angle distribution of the selected showers is consistent with exponential atmospheric absorption with an absorption length of 150 ± 5 g cm^{-2}.

The results show no indication of a change in the slope of the primary cosmic-ray energy spectrum within the energy range 10^{17}–10^{18} ev.

1. Introduction

Current interest in the primary cosmic-ray energy spectrum at high energies centres on two regions. One region is marked by a reduction in the slope of the primary energy spectrum in the vicinity of 10^{18} ev, and possibly corresponds to a transition of the primary radiation from predominantly heavy nuclei of galactic origin to protons of extragalactic origin (Linsley 1963). The other region corresponds to the position of a predicted rapid cut-off of the primary proton energy spectrum around 10^{20} ev caused by the interaction of primary protons with the postulated universal black-body radiation (Greisen 1966). More recent calculations suggest that the cut-off would commence at $10^{19\cdot5}$ ev for protons and at even lower energies for heavy nuclei (Hillas 1968).

In addition to the large air shower arrays at Chacaltaya (Bradt *et al.* 1965), Sydney (Brownlee *et al.* 1968), Moscow (Vernov and Khristiansen 1967) and Haverah Park (Earnshaw *et al.* 1968), a number of other experiments have been designed to study air showers initiated by primary cosmic rays with energies in these regions (Matano *et al.* 1968, Bunner *et al.* 1968).

The measurements of the energy-loss spectrum presented here complement an earlier study of the celestial arrival directions of the same showers (Blake *et al.* 1968), and refer to energies close to the transition value reported by Linsley.

2. Experimental details

The Haverah Park 500 m extensive air shower array consists of three water-filled Čerenkov detectors, each of area 34 m^2 and depth 1·2 m, symmetrically disposed at a radius of 500 m about a similar central detector. The mean altitude of the array is 220 m above sea level. Measurements of the arrival times and energy-loss densities are made at each of the four detectors. A description of the array has been given elsewhere (Tennent 1967).

†Now at Tata Institute of Fundamental Research, Bombay, India.

Approximately 30 000 showers were recorded by the array between July 1963 and the end of June 1966 in a total running time of $6{\cdot}4 \times 10^7$ s. About 10% of these showers (2950) were selected for inclusion in the energy-loss spectra.

3. Energy-loss density of an air shower

When an air shower falls on a Čerenkov detector of the type used at Haverah Park, the signal produced by the detector is proportional to an 'energy-loss surface density' (Mev m^{-2}) equal to the energy lost by a shower in 1·2 m of water, measured in the direction of the shower axis, per unit area normal to the shower axis. This we call the *energy-loss density* of the shower.

To a first approximation, the constant of proportionality relating energy-loss density to detector signal is the same for both the muon component and the electron–photon component of an air shower and is independent of the inclination of the axis of the shower for zenith angles up to about 40°.

These points have been discussed elsewhere (Hollows 1968), but briefly they follow from the size and the shape of the Haverah Park detectors, which are such that few muons stop in a detector, whereas almost the entire electron–photon component is stopped. Also the surface area presented to a shower by a detector is roughly constant and equal to the horizontal area of the detector up to zenith angles of about 40°.

Although the energy-loss density of a shower can be related to the more familiar shower properties measured by charged-particle detectors, the relations, taken in isolation, are not helpful. For example, under certain conditions the energy-loss density of a shower is proportional to the number density (m^{-2}) of the muon component and the energy density (Mev m^{-2}) of the electron–photon component. The relative weights of the contributions of the two components to the energy-loss density are roughly in the ratio of two to one. A more fruitful approach is simply to regard the energy-loss density (Mev m^{-2}) as the shower property measured by Čerenkov detectors of the type used at Haverah Park in the same way that the charged-particle density (m^{-2}) is the shower property measured by thin-walled Geiger counters or very thin scintillators.

The parameter obtained by summing the energy-loss density of a shower over a specified range of core distances is termed the energy loss of the shower. The sum between core distances of 100 m and 1000 m for near-vertical showers at sea-level represents about 1% of the energy of the primary cosmic ray that initiated the shower (Suri 1965).

Energy loss is the parameter used by us to compare different showers recorded by Čerenkov detectors; in this restricted sense energy loss is analogous to shower size. However, the fluctuations in the energy loss of showers initiated by primary cosmic rays of given energy and mass are expected to be smaller than the corresponding fluctuations in shower size.

4. Shower analysis

4.1. *Energy loss* E_{100}

Over the range of core distances $100 < r < 1000$ m, determined in part by the array geometry, the lateral distribution of the energy-loss density of a shower can be represented by a power law $\Delta(r) = Kr^{-n}$. Showers may be compared by introducing an *energy loss* E_{100}, defined by

$$E_{100}(K, n) = \int_{100}^{1000} 2\pi r \Delta \, \mathrm{d}r. \tag{1}$$

The limits of the integral defining energy loss correspond to the range of distances over which the array was capable of measuring energy-loss densities.

4.2. *Initial shower analysis*

The four energy-loss densities and the arrival direction of the shower uniquely determine a set of values for K, X, Y and n for the shower, where $(X, Y, 0)$ are the coordinates of the intersection of the shower axis and the horizontal plane through the central detector. Each shower is characterized by unique values for both the exponent n and the energy loss E_{100} in this method of shower analysis.

4.3. *Least-squares shower analysis*

Showers in given intervals of energy loss and zenith angle show a wide distribution of values of n which arises principally from statistical fluctuations of the measured densities at the four detectors, particularly from the uncertainty as to the value of the smallest of the densities. A more reliable set of values for K, X and Y is given by a weighted least-squares re-analysis of all the showers falling in a given interval of energy loss and zenith angle, using a constant power law exponent in the analysis equal to the median of the distribution of values of n for all showers in the interval. The median of this distribution of values of the exponent n is referred to as the *median exponent* and is denoted by m. It should be stressed that the energy loss obtained on re-analysis by the method of least squares depends on the value of m, in addition to the four energy-loss densities and the arrival direction of the shower. However, each shower is still characterized analytically by a particular value of n.

5. Selection criteria for showers

The array detects showers which have energy-loss densities at three or more detectors that exceed a pre-determined trigger level equal to 70 Mev m^{-2} set by the recording equipment. The trigger level was the same for all four detectors.

Those showers that trigger the array are a biased sample of the shower population owing to fluctuations of the energy-loss densities about the trigger levels and the fact that the energy-loss spectrum falls steeply with increasing energy loss.

To reduce this bias, a selection condition was applied to showers which triggered the array. Only those showers for which three or more energy-loss densities exceeded the trigger level by three or more standard deviations were selected for inclusion in the energy-loss spectra. This means that the densities had to exceed 110 Mev m^{-2}.

The densities to which the selection condition was applied were not the directly observed values, but ones recalculated after the coordinates of the core and the energy loss of the shower had been obtained from a least-squares analysis of the data using the appropriate value of the median exponent.

Showers included in the energy-loss spectra were subject to three further conditions which ensured that the arrival directions and the core positions could be calculated with satisfactory precision for all showers on a consistent basis. The conditions were that the arrival times at all three outer detectors were known, and that the perpendicular distance of the shower core was (i) less than 500 m from the central detector and (ii) greater than 150 m from each of the detectors.

Finally, showers included in the energy-loss spectra were restricted to those for which the energy-loss densities were proportional to the signal from the Čerenkov detectors, i.e. to showers with zenith angles less than 40° (§ 3).

6. Dependence of the median exponent on zenith angle and energy loss

The observed variation of the median exponent $m(\theta)$ with zenith angle θ, for all values of energy loss, may be represented by

$$m(\theta) = 6{\cdot}37 - 4{\cdot}56 \sec(\theta) + 1{\cdot}45 \sec^2(\theta) - 0{\cdot}15 \sec^3(\theta) \tag{2}$$

for $0° < \theta < 55°$. This relation is shown plotted in figure 1.

In the angular range 0°–40° the median exponent varies by 0·5. No significant variation of m with θ was found within each of the zenith angle ranges 0°–20°, 20°–30°, 30°–35° and 35°–40°, and for the purposes of calculation m was regarded as a constant within a given range.

The variation of the median exponent $m(E_{100}; \theta)$ with energy loss E_{100} within the four zenith angle intervals was obtained by the method of successive approximations because the energy loss of a shower itself depends on the value of m used to calculate E_{100}. The iteration used to generate successive approximations was the same for each of the four zenith angle ranges mentioned above.

The E_{100} values used to start the first iteration were the set obtained by analysing all showers in a given zenith angle interval by the method of least squares, using a constant exponent to ensure that no spurious energy-loss dependence was introduced at the outset. The values of the exponent used for the four zenith angle intervals were 3·0, 2·9, 2·8 and 2·7, respectively.

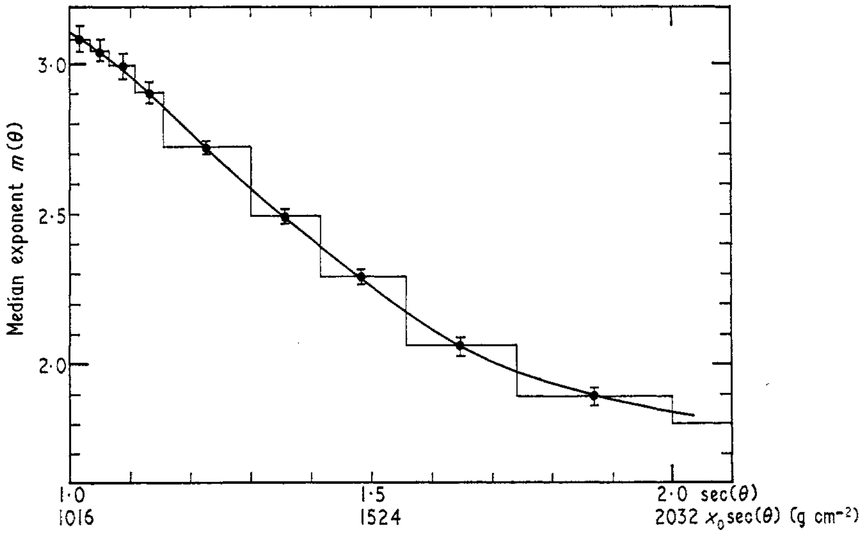

Figure 1. Variation of the median exponent $m(\theta)$ with zenith angle θ for all values of energy loss E_{100}.

Each iteration consisted of the following steps. Energy-loss values entering the iteration were grouped in equal logarithmic intervals and the median exponent $m(E_{100})$ calculated for each energy-loss interval from the distribution of values of the exponent n for showers with E_{100} falling in that interval. These values of $m(E_{100})$ represent successive approximations to the required dependence of the median exponent on energy loss.

The remainder of the iteration generated a new set of energy-loss values E'_{100}, by re-determining the energy loss for each shower from a complete least-squares analysis of the shower, using the value of $m(E_{100})$ obtained from the current approximation, and thus completed the iteration.

Two cycles of the iteration were sufficient. The dependence of the median exponent on energy loss obtained in this way can be represented by

$$
\begin{aligned}
m(E_{100}) &= (3\cdot05 \pm 0\cdot02) + (0\cdot50 \pm 0\cdot03) \lg \left(\frac{E_{100}}{10^{15}}\right) && 0^\circ < \theta < 20^\circ \\
m(E_{100}) &= (2\cdot93 \pm 0\cdot02) + (0\cdot30 \pm 0\cdot03) \lg \left(\frac{E_{100}}{10^{15}}\right) && 20^\circ < \theta < 30^\circ \\
m(E_{100}) &= (2\cdot80 \pm 0\cdot02) + (0\cdot18 \pm 0\cdot02) \lg \left(\frac{E_{100}}{10^{15}}\right) && 30^\circ < \theta < 35^\circ \\
m(E_{100}) &= (2\cdot70 \pm 0\cdot04) && 35^\circ < \theta < 40^\circ
\end{aligned}
\qquad (3)
$$

for $10^{14\cdot6} < E_{100} < 10^{15\cdot6}$ ev, and these results are shown in figure 2.

The final estimate of the energy loss of individual showers was based on a least-squares analysis, using a value of the median exponent which took into account the dependence of the median exponent on both zenith angle and energy loss.

7. Acceptance area of the array

Following Clark *et al.* (1961), we define an *acceptance area* $A(E_{100})$ for the array as an area over which the probability of detecting showers of energy loss E_{100} is substantially unity. Showers whose cores fell in the acceptance area and which satisfied the selection criteria discussed in § 5 were used to determine the energy-loss spectra. The definition of the acceptance area is conveniently stated in two parts.

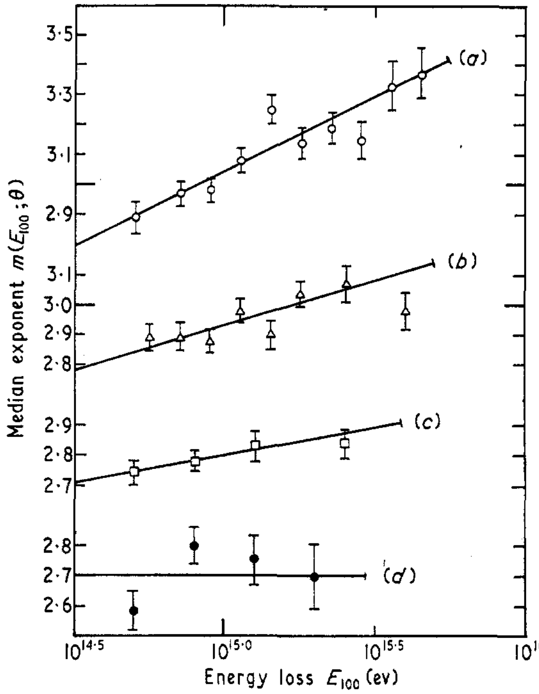

Figure 2. Variation of the median exponent $m(E_{100};\,\theta)$ with energy loss E_{100} for zenith angle intervals (*a*) 0°–20°, (*b*) 20°–30°, (*c*) 30°–35° and (*d*) 35°–40°.

The first part involves only the array geometry and the shower arrival direction. Suppose (i) that the array is projected on a plane normal to the arrival direction of a shower, (ii) that circular arcs of radius r_0 are drawn about each outer detector in the plane of projection and (iii) that $A'(r_0)$ is the area in the plane of projection enclosing points distant r_0 or less from any two of the three outer detectors. Then the required area $A(r_0)$ is obtained from the area A' by excluding from A' those regions in the plane of projection which lie outside a circle of radius 500 m about the central detector or inside circles of radius 150 m about each detector, where the circles are also drawn in the plane of projection.

It remains to determine the appropriate value of r_0. The detection probability for showers is sufficiently close to unity for our purpose if the energy-loss densities at three or more detectors exceed the trigger level by three or more standard deviations (§ 5). Hence setting the distance r_0 equal to

$$r_0 = \left\{\frac{(m-2)E_{100}/\Delta_0}{2\pi(100^{2-m}-1000^{2-m})}\right\}^{1/m} \tag{4}$$

completes the definition of the acceptance area $A(E_{100};\,\theta,\,\phi)$ for a shower of energy loss E_{100}, median exponent m, arrival direction $(\theta,\,\phi)$ and a selection level Δ_0 equal to 110 Mev m^{-2} at each detector.

The acceptance area of the array was measured with a planimeter from scale drawings of the projected array for selected zenith angles, azimuths and values of the parameter r_0. The acceptance area is independent of azimuth for vertical showers and varies with azimuth by only a few per cent, even for steeply inclined showers, because of the geometrical symmetry of the arms of the array.

8. Energy-loss spectrum of air showers

Showers satisfying the selection criteria were grouped in intervals of zenith angle, and within each zenith angle interval in equal logarithmic intervals of energy loss, and the acceptance area $A(E_{100};\ \theta)$ calculated for each shower. The differential energy-loss spectrum for each zenith angle interval was obtained by assigning a statistical weight equal to $1/T\Omega A$ to each shower, summing the weights for showers in a given energy-loss interval and plotting the resulting sum, divided by the size of the energy-loss interval, as a function of the mean energy loss for the interval. Here T and $\Omega(\theta)$ are the array running time and the solid angle corresponding to the zenith angle interval respectively. The corresponding integral energy-loss spectra, shown in figure 3, for the zenith angle intervals 0°–20°, 20°–30°, 30°–35° and 35°–40°, are based on a sample of 2950 showers which satisfied the selection criteria, i.e. had cores falling in the acceptance areas.

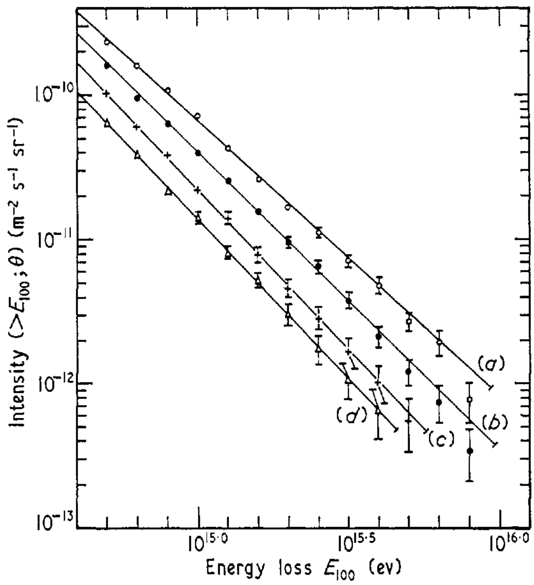

Figure 3. Integral intensity E_{100} energy-loss spectra for zenith angle intervals (*a*) 0°–20°, (*b*) 20°–30°, (*c*) 30°–35° and (*d*) 35°–40°.

Each of the four integral energy-loss spectra may be represented by a power law of the form

$$I(>E_{100},\bar{x}) = I_{15}(\bar{x})\left(\frac{E_{100}}{10^{15}}\right)^{-\gamma} \qquad (m^{-2}\ \mathrm{s}^{-1}\ \mathrm{sr}^{-1}) \tag{5}$$

for $10^{14\cdot6} < E_{100} < 10^{15\cdot6}$ ev, where $\bar{x}$ is the mean atmospheric depth corresponding to the zenith angle interval, $I_{15}(\bar{x})$ is the intensity of showers with $E_{100} > 10^{15}$ ev and γ is the slope of the integral energy-loss spectrum. Values of $\bar{x}$, $I_{15}(\bar{x})$ and γ for each of the zenith angle intervals are given in table 1.

Table 1

θ (deg)	x (g cm^{-2})	$I_{15}(\bar{x})$ (10^{-11} m^{-2} s^{-1} sr^{-1})	γ
0–20	1049	$6\cdot6 \pm 1\cdot3$	$1\cdot94 \pm 0\cdot06$
20–30	1127	$4\cdot0 \pm 0\cdot8$	$2\cdot10 \pm 0\cdot06$
30–35	1207	$2\cdot2 \pm 0\cdot5$	$2\cdot26 \pm 0\cdot09$
35–40	1283	$1\cdot4 \pm 0\cdot3$	$2\cdot22 \pm 0\cdot10$

9. Zenith angle distribution of air showers

The zenith angle distributions shown in figure 4 were obtained by grouping showers satisfying the selection criteria into four intervals in energy loss: $8 \cdot 0 \times 10^{14}$–10^{15}, 10^{15}–$1 \cdot 3 \times 10^{15}$, $1 \cdot 3 \times 10^{15}$–$2 \cdot 0 \times 10^{15}$ and greater than $2 \cdot 0 \times 10^{15}$ ev. Within each of these intervals the showers were sub-divided into five equal intervals ($\Delta x = 62 \cdot 5$ g cm^{-2}) of atmospheric depth x. A statistical weight equal to $1/A(E_{100}, x)$ was assigned to each shower, where A is the acceptance area for the shower, $x = x_0 \sec(\theta)$ and $x_0 = 1016$ g cm^{-2}. The sum of the weights of the showers in a given interval divided by the corresponding element of solid angle $\Delta\Omega = 2\pi(x_0/x^2)\Delta x$ is proportional to the ordinate of the zenith angle distribution for the interval.

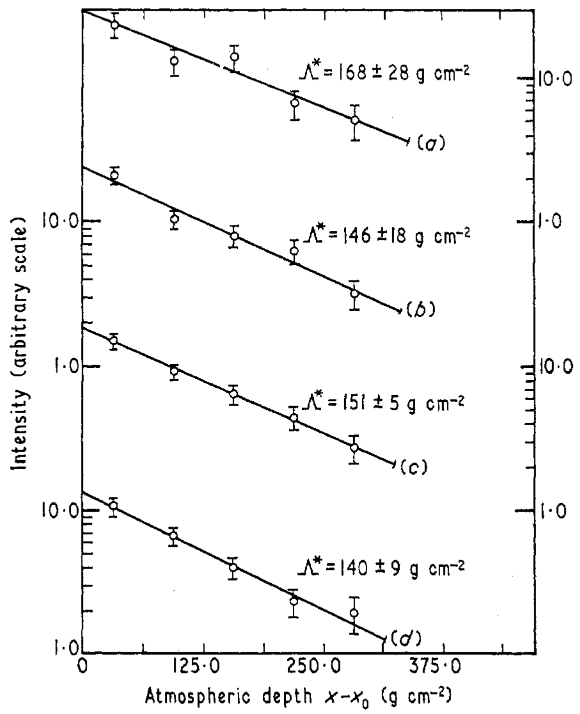

Figure 4. Zenith angle distributions for energy-loss intervals (*a*) 8×10^{14}–10^{15}, (*b*) 10^{15}–$1 \cdot 3 \times 10^{15}$, (*c*) $1 \cdot 3 \times 10^{15}$–2×10^{15} and (*d*) $> 2 \times 10^{15}$ ev, where $x = x_0 \sec(\theta)$ and $x_0 = 1016$ g cm^{-2}.

The four distributions are each exponential in form and all four are consistent with a single value for an absorption length $\Lambda^* = 150 \pm 5$ g cm^{-2}, although there is a suggestion, which is not statistically significant, that Λ^* decreases with increasing energy loss.

A direct comparison of Λ^* with the conventional shower absorption length $\Lambda = -\partial \ln\{I(>N, x)\}/\partial x$, where $I(>N, x)$ is the integral size spectrum at an atmospheric depth x, would be misleading because the quantity we measure is $\Lambda^* = -\partial \ln\{I(>E_{100}, x)\}/\partial x$, where $I(>E_{100}, x)$ is the integral E_{100}–energy-loss spectrum at a depth x, and $E_{100} = FE$. The fraction F of the total energy loss E that falls in the range of core distances $100 < r < 1000$ m will itself vary with depth.

The three energy-loss spectra for inclined showers have not been used to extend the range of the spectrum for near-vertical showers using the effective solid angle method (Clark *et al.* 1961) because of the possibility that Λ^* depends on E_{100}.

10. Discussion

10.1. *Shower composition*

The values of the median exponent shown in figures 1 and 2 range from 3·1 to 1·9 with zenith angle and from 2·7 to 3·4 with energy loss. These changes may arise from changes in

(i) the lateral distribution of the muons in showers, or (ii) the lateral distribution of the energy flow of the electron–photon component (§ 3) or (iii) the composition of the showers, i.e. the proportion of electrons and photons to muons in the shower. We show below that changes in the lateral distributions are not sufficient to account for the observed variation of the median exponent.

An earlier experiment at Haverah Park (Allan *et al.* 1968) showed that the exponent of the lateral distribution of the muon component changed slowly with zenith angle from about 2·2 for near-vertical showers to about 1·9 for showers inclined at angles in excess of 60°, and that the exponent was independent of energy loss.

The lateral distribution of electrons in air showers is almost invariant with respect to zenith angle and shower size, and therefore with respect to energy loss. The form of the lateral distribution is in broad agreement with the average distribution computed for a pure electromagnetic cascade not very far from the stage at which the number of particles is a maximum.

The lateral distribution of energy flow in an electromagnetic cascade, defined as the energy in an annular ring $(r, r+dr)$, is $1/r$ times steeper than the lateral spread of the electrons in the cascade for core distances of less than 100 m. Beyond 100 m the average energy in the electron–photon component, per electron, becomes roughly constant and the lateral distribution of energy flow follows the lateral spread of the electrons. The lateral distribution of the energy flow of the electron–photon component of air showers is therefore also substantially invariant with respect to zenith angle and energy loss.

However, at core distances typical of showers recorded by the Haverah Park 500 m array, i.e. from 300–500 m, the exponents of the lateral distributions of the energy density of the electron–photon component and of the number density of the muon component are very different in value, about 4 and 2, respectively. The observed variation of the median exponent may be attributed in the main to changes in the proportion of electrons to muons with zenith angle and energy loss. In particular, where the value of the median exponent closely approaches the value of the exponent of the lateral distribution of muons, as it does for very inclined showers, it is known that muons are responsible for nearly the whole of the signal from the Čerenkov detectors (Allan *et al.* 1968).

The change in the median exponent with zenith angle corresponds predominantly to a decrease in the proportion of the electron–photon component with increasing atmospheric depth, and the change with energy loss to an increase in the proportion of the soft component as the depth of shower maximum increases with increasing primary energy.

Linsley (1963) has reported a similar energy dependence for the exponent of the lateral distribution of charged particles from Volcano Ranch, where the range of core distances over which measurements were made was comparable with that at Haverah Park. We interpret these results to mean that the two arrays, although at different depths in the atmosphere, sampled showers at core distances at which the effects of changes in composition on the lateral distribution were roughly comparable.

By contrast, no such energy dependence was reported from two smaller arrays (Clark *et al.* 1961, Delvaille *et al.* 1960), where the measurements referred to smaller core distances on average, i.e. to distances at which the proportion of muons to electrons was much smaller.

10.2. *Minimum core distance*

The number, area and the separation of the detectors of an air shower array, the dynamic range of the recording system and the selection criteria applied to the recorded showers together effectively set upper and lower limits, R_2 and R_1, on the range of core distances over which an array is capable of measuring a charged-particle density or an energy-loss density. As a result an array can only measure a certain fraction F of the total shower size N or of the total energy loss E. If the structure function is the same for all shower sizes or for all energy losses $F = F(R_1, R_2)$ alone and the distribution of FN or of FE measured by the array is identical with the distribution of N or of E apart from a trivial scale change. If the form of the structure function outside the region $R_1 < r < R_2$ is known from some other source, F may be calculated. These results are well known and we mention them in passing only because the situation is different when the structure function is not the same for showers of all sizes or of all energy losses, for then $F = F(R_1, R_2, N)$ or $F = F(R_1, R_2, E)$ and the distribution of FN or of FE measured by the array is no longer identical with that of N or of E.

We have had to restrict our estimate of the energy loss of a shower to the range $100 < r < 1000$ m because we do not know the form of the structure function for energy-loss density outside this range, i.e. we cannot calculate F, and in addition the structure function depends on energy loss, i.e. $F = F(R_1, R_2, E)$, which means that the distribution of FE measured by the Haverah Park array differs from that for E.

In our case the variation of the median exponent with energy loss means that the slope γ of the integral energy-loss spectrum depends on the values of the two core distances R_1 and R_2 chosen for the limits of the integral defining energy loss (equation (1)). In the absence of such an energy-loss dependence γ does not depend on R_1 or R_2. The dependence of γ on R_1 and R_2 complicates both the interpretation of the relation between the slope of the integral energy-loss spectrum and the slope of the primary energy spectrum, and also the comparison of the energy-loss spectra obtained by arrays of similar geometry but dissimilar size.

An indication of the extent of the variation of γ with minimum core distance R_1, for a fixed maximum core distance $R_2 = 1000$ m, is given in table 2 for showers with zenith angle less than 20°.

Table 2

R_1 (m)	100	200	300	400	500	600
γ	1·94	2·19	2·36	2·52	2·62	2·76

The lower limit we have chosen ($R_1 = 100$ m) corresponds to the smallest core distance on average at which energy-loss densities can be measured by the Haverah Park 500 m array. The corresponding figure for the Haverah Park 2 km array lies between 200 and 400 m.

10.3. *Energy-loss spectrum for near-vertical showers*

The energy-loss spectrum for near-vertical showers is shown in figure 5. For interest we have also plotted the energy-loss spectrum derived from the initial analysis of the same

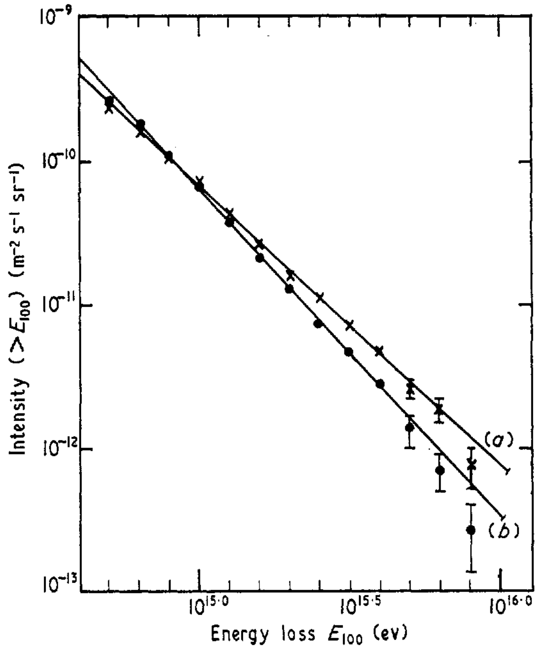

Figure 5. Integral intensity E_{100} energy-loss spectra for near-vertical showers obtained by using a median exponent (*a*) with and (*b*) without energy-loss dependence.

showers using a median exponent without energy-loss dependence. The slope of the latter spectrum is $2{\cdot}28 \pm 0{\cdot}06$ as opposed to $1{\cdot}94 \pm 0{\cdot}06$. The effect of the energy-loss dependence of the exponent is to flatten the slope of the integral energy-loss spectrum.

A similar effect was observed by Linsley, who reported that the slope of the shower size spectrum changed from 2·26 to about 2·0, for primary energies of about 10^{17} ev, when the size dependence of the structure function was taken into account in the shower analysis (Linsley *et al.* 1962, Linsley 1963).

10.4. *Energy loss and primary energy*

The method used to relate the energy loss of a shower to the energy of the primary that initiated the shower is analogous to the method used to relate shower size N to primary energy; both methods involve the calculation of a conversion factor $C(E_p, A)$ as a function of the energy E_p and mass number A of the primary, such that

$$E_p = C_{100}E_{100} \qquad \text{or} \qquad E_p = CN$$

from models of shower development in the atmosphere.

Baxter (1969) has carried out a cascade calculation describing the average development of an air shower initiated by a proton of energy $9{\cdot}0 \times 10^{16}$ ev. The calculation took into account the characteristic properties of the Čerenkov detectors used at Haverah Park; it showed that $C_{100} = 1{\cdot}6 \times 10^2$. The primary intensity calculated from this value of C_{100} and the integral energy-loss spectrum for near-vertical showers is in agreement with the intensity calculated from the Chacaltaya primary energy spectrum (Bradt *et al.* 1965).

It is not possible to derive a primary energy spectrum from our energy-loss measurements because neither the extent to which C_{100} depends on E_p and A, nor the mass composition of primaries with energies in the interval 10^{17}–10^{18} ev is known at present. Primary compositions ranging from $A = 1$ (Linsley and Scarsi 1962) to $A > 10$ (Orford and Turver 1968) have been suggested for the interval.

However, these measurements do enable an upper limit to be placed on a possible change in the slope of the primary energy spectrum within the interval 10^{17}–10^{18} ev. The argument developed below is briefly as follows.

(i) The energy-loss measurements presented here are related in a simple way (a power law relation) to existing measurements of the size spectrum of showers at Chacaltaya and Volcano Ranch. Our energy-loss measurements may be regarded as an extension of these earlier size measurements of showers near the depth of maximum longitudinal development.

(ii) The conversion factor $C_m(E_p, A)$ from size at shower maximum to primary energy E_p is almost independent of E_p and is insensitive to A. Consequently, the primary energy spectrum inferred from a size spectrum at shower maximum is not significantly influenced by uncertainties as to the mass composition of the primaries.

10.4.1. *The Chacaltaya primary energy spectrum.*

This spectrum shown in figure 6 was derived in effect from a charged particle size spectrum for showers at maximum development using a *constant* conversion factor $C_m = 2{\cdot}0 \times 10^9$ ev/shower particle, which was consistent with estimates based on various models of shower development for showers initiated by proton primaries. The corresponding size spectrum at shower maximum may therefore be recovered from the Chacaltaya primary energy spectrum shown in figure 6 simply by re-labelling the axes. The Volcano Ranch primary energy spectrum (Linsley 1963) also refers to showers near the depth of maximum longitudinal development, and the value of the conversion factor used to calculate the Volcano Ranch energy spectrum from the size spectrum was the same as that used at Chacaltaya.

Inspection of figure 6 indicates that the quantities measured at Chacaltaya and Haverah Park, shower size at shower maximum N_m and energy loss at sea level E_{100}, respectively, are related by

$$N_m = K(E_{100})^{\alpha} \tag{6}$$

over the range of intensities in which the two sets of measurements overlap, where K and α are constants. A similar relation exists between the Volcano Ranch shower size measurements and the Haverah Park energy-loss measurements, with different values for K and α, over an intensity range which overlaps the Chacaltaya measurements.

In the range of intensities common to the Chacaltaya and Volcano Ranch measurements the differences between the values of K or α arise either from the way in which the data obtained from the two experiments have been analysed or from the difference in the depths of the two arrays (530 and 820 g cm^{-2} respectively), depending on whether one regards the graphs as graphs of the primary energy spectrum or as graphs of shower size spectra. The differences do not indicate that K or α is changing with shower size or primary energy.

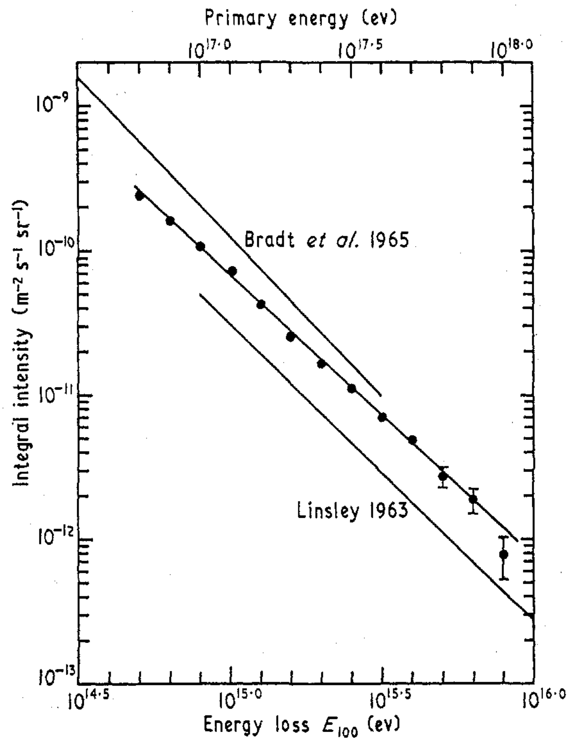

Figure 6. The range of intensities common to the present measurements of energy loss and the Chacaltaya and Volcano Ranch primary energy spectra (Bradt *et al.* 1965, Linsley 1963).

The three sets of measurements, taken together, indicate that there is no change in K or α over the entire intensity range of the Haverah Park measurements. We suppose therefore that

$$E_{\mathrm{p}} = C_{\mathrm{m}}N_{\mathrm{m}} = C_{\mathrm{m}}K(E_{100})^{\alpha} \tag{7}$$

and that K and α are constant. The Haverah Park energy-loss measurements may therefore be regarded as an extension of the Chacaltaya size measurements at shower maximum or of the Volcano Ranch measurements.

10.4.2. *The conversion factor for proton initated showers.* This factor for showers near maximum development is almost independent of primary energy:

$$C_{\mathrm{m}}(E_{\mathrm{p}}, 1) = 1{\cdot}73 \times 10^{9} \left(\frac{E_{\mathrm{p}}}{10^{14}}\right)^{-0{\cdot}03} \text{ ev/shower particle} \tag{8}$$

for $10^{14} < E_{\mathrm{p}} < 5{\cdot}0 \times 10^{17}$ ev. Equation (8) is consistent with figures 5(*a*) and 5(*b*) of La Pointe *et al.* (1968) and with the relation $(E_{\mathrm{p}}/10^{14}) = 1{\cdot}7(N/10^{5})^{0{\cdot}97}$.

The conversion factor for showers initiated by primaries heavier than protons is insensitive to both E_{p} and A. The ratio of the conversion factors for iron nuclei and protons for example, $C_m(E_p, 56)/C_m(E_p, 1)$, decreases from $1{\cdot}8 \pm 0{\cdot}5$ at 10^{14} ev to $1{\cdot}4 \pm 0{\cdot}6$ at 10^{16} ev. These figures have been taken from table 2 of Bradt and Rappaport (1967). In the calculation described below we have assumed that this ratio is about 1·4 for $10^{17} < E_p < 10^{18}$ ev, and that both the ratio and the conversion factor for protons do not change with primary energy.

To obtain an upper limit on possible changes in the primary energy spectrum that may arise from uncertainties in mass composition, we first suppose that the primary mass composition changes abruptly from protons to iron nuclei or vice versa at some particular shower size or energy loss, and calculate the corresponding primary energy spectrum from the conversion factors given above and the continuous power law size or energy-loss spectrum that represents the observations at Chacaltaya or Haverah Park.

We next suppose that the same overall change in primary composition takes place in a succession of discrete changes distributed in an arbitrary way over a finite interval in shower size or energy loss, and use the results obtained above to calculate the change in the slope of the primary energy spectrum within the energy range that corresponds to the shower size interval.

Finally, by making an appropriate choice for the size of the interval over which we suppose the composition change to have taken place, we may interpret the change in the slope of the primary energy spectrum as the uncertainty arising from the lack of knowledge of the primary mass composition.

The first part of the calculation described above shows that the effect of an abrupt change in primary composition from protons to iron nuclei (or vice versa) is simply to displace the graph of primary integral intensity against primary energy up (or down) by a factor of $(1{\cdot}4)^{\gamma} \simeq 2$ for energies above a transition region whose width is equal to a factor of 1·4 in energy. The transition region is bounded by the two primary energies that correspond to the shower size at which the composition change is supposed to occur. Outside the transition region the slope of the graph remains everywhere the same as that of the size spectrum γ, where $\gamma = -\partial \ln I(>N)/\partial \ln N$.

The second part of the calculation shows that the fractional change in the slope of the primary energy spectrum is given by $\ln R/\ln Q$, where R is the ratio of the conversion factors corresponding to an overall composition change that takes place between energies E and QE.

Finally, if we assume that the composition change corresponds to a rigidity cut-off, i.e. we suppose that the primary composition changes from protons to iron nuclei, say between energies E and $26E$, we have $R = 1{\cdot}4$, $Q = 26$ and $\ln R/\ln Q \simeq 0{\cdot}1$. This figure is comparable with the uncertainty in the slope of the Chacaltaya size spectrum (7%) or the Haverah Park energy-loss spectrum (3%).

Alternatively, if we assume that the composition changes from iron nuclei of galactic origin to protons of extragalactic origin and suppose for simplicity that the change occurs abruptly, the fractional change in slope of the primary energy spectrum is zero outside a transition region whose width is a factor 1·4 in energy. Thus changes in primary composition seem unlikely to influence the slope of the primary energy spectrum derived from a power-law size or energy-loss spectrum by an amount which exceeds the present statistical uncertainties.

Primaries of a given energy can give rise to showers whose sizes vary widely from the average size even at shower maximum. It remains to consider whether fluctuations in shower size influence the conclusion reached above concerning the slope of the primary energy spectrum.

If the width of the distribution of shower size N for a fixed primary energy E_p is defined as the range of N which contains 90% of the showers, the calculations of Bradt and Rappaport (1967), for proton and iron primaries in the energy range 10^{14}–10^{16} ev, indicate that the widths of the distributions at shower maximum are factors of 2·5 and 1·5, respectively, in shower size. The widths of the distributions are independent of primary energy in the two cases.

The distribution of $\ln N$ appears to be roughly normal, i.e. N is log-normally distributed about a mean shower size $\bar{N}$. If this is indeed the case and it is assumed that $\bar{N} \propto E_p{}^{\beta}$, then it can be shown that a power law primary energy spectrum of slope $w \equiv -\mathrm{d}\ln I(>E_p)/\mathrm{d}\ln E_p$ gives rise to a power law size spectrum whose slope is w/β, where w and β are constants. The same slope results if the fluctuations in shower size for a fixed primary energy are negligible.

However, in order to assert that the primary energy spectrum continues without a change of slope up to an energy E_p in the presence of fluctuations in shower size, it is necessary that the corresponding shower size spectrum continues without a change of slope up to a size of about $\sqrt{2}\bar{N}$. The Haverah Park energy-loss measurements extend to primary energies of about 10^{18} ev. We conclude from these measurements alone that there is no indication of a discontinuous change in the slope of the primary energy spectrum up to an energy of about 7×10^{17} ev. If the Haverah Park measurements are combined with those of Volcano Ranch, which show no pronounced discontinuity in the differential size spectrum up to about $N_m \simeq 10^9$, i.e. $E_p \simeq 2\times10^{18}$ ev, the upper limit is raised to about 10^{18} ev.

11. Conclusion

The integral E_{100} energy-loss spectrum of near-vertical air showers may be represented by a power law of constant exponent $-1{\cdot}94\pm0{\cdot}06$ over the energy-loss range $5\times10^{14} < E_{100} < 6\times10^{15}$ ev, which corresponds, in so far as the relation between energy loss and primary energy has been established, to primary energies within the range 10^{17}–10^{18} ev.

Subject to the reservation above, the results show no indication of a change in the slope of the primary energy spectrum in this energy range, in agreement with results reported by Linsley (1963) and Bradt *et al.* (1965).

In an earlier study of these same showers Blake *et al.* (1968) concluded that no indication existed of an anisotropic distribution of the arrival directions of the showers. This conclusion, taken in conjunction with the results presented here, suggests that no great change is taking place in the acceleration mechanism, the effective source distribution or the containment mechanism of the primary radiation in this energy range.

Acknowledgments

The authors would like to acknowledge their indebtedness to Professor J. G. Wilson and the Science Research Council, for the provision of facilities for this work, the Science Research Council, for a maintenance grant to J.D.H., and the Association of Commonwealth Universities for a Commonwealth Scholarship for A.N.S. They would also like to thank their colleagues in the Haverah Park group at Leeds for the operation of the array and the collection of the data discussed here, and past and present members of the Haverah Park groups in Leeds, Durham and Imperial College, London, and Dr. A. M. Hillas of the University of Leeds, for help received in discussions.

References

Allan, H. R., Blake, P. R., Neat, K. P., and Pidcock, J. K., 1968, *Can. J. Phys.*, **46**, S98–101.

Baxter, A. J., 1969, *J. Phys.* A (*Gen. Phys.*), [2], **2**, 50–8.

Blake, P. R., *et al.*, 1968, *Can. J. Phys.*, **46**, S78–80.

Bradt, H. V., *et al.*, 1965, *Proc. 9th Int. Conf. Cosmic Rays, London*, Vol. 2 (London: Institute of Physics and Physical Society), pp. 715–7.

Bradt, H. V., and Rappaport, S. A., 1967, *Phys. Rev.*, **164**, 1567–83.

Brownlee, R. G., *et al.*, 1968, *Can. J. Phys.*, **46**, S259–62.

Bunner, A. N., Greisen, K., and Landecker, P. B., 1968, *Can. J. Phys.*, **46**, S266–9.

Clark, G. W., *et al.*, 1961, *Phys. Rev.*, **122**, 637–54.

Delvaille, J., Kendziorski, F., and Greisen, K., 1960, *Proc. 6th Moscow Cosmic Ray Conf., Moscow*, Vol. 2 (Moscow: State Publishing House), pp. 79–83.

Earnshaw, R. A., *et al.*, 1968, *Can. J. Phys.*, **46**, S5–8.

Greisen, K., 1966, *Phys. Rev. Lett.* **16**, 748–51.

Hillas, A. M., 1968, *Can. J. Phys.*, **46**, S623–6.

Hollows, J. D., 1968, *Ph.D. Thesis*, University of Leeds.

La Pointe, M., *et al.*, 1968, *Can. J. Phys.*, **46**, S68–71.

LINSLEY, J., 1963, *Proc. 8th Int. Conf. Cosmic Rays, Jaipur*, Vol. 4 (Bombay: Commercial Printing Press), pp. 77–99.
LINSLEY, J., and SCARSI, L., 1962, *Phys. Rev. Lett.* **9**, 123–5.
LINSLEY, J., SCARSI, L., and ROSSI, B., 1962, *J. Phys. Soc. Japan* (*Suppl.* A3), **17**, 91–102.
MATANO, T., NAGANO, M., SUGA, K., and TANAHASHI, G., 1968, *Can. J. Phys.* **46**, S255–8.
ORFORD, K. J., and TURVER, K. E., 1968, *Nature, Lond.*, **219**, 706–8.
SURI, A. N., 1965, *Proc. 9th Int. Conf. Cosmic Rays, London*, Vol. 2 (London: Institute of Physics and Physical Society), pp. 751–3.
TENNENT, R. M., 1967, *Proc. Phys. Soc.*, **92**, 622–31.
VERNOV, S. N., and KHRISTIANSEN, G. B., 1967, *Proc. 10th Int. Conf. Cosmic Rays, Calgary*, Part A (Calgary: University of Calgary Press), pp. 345–96.